CONCEPTUAL DESIGN OF A HYBRID (TURBOFAN/SOLAR) POWERED HALE UAV

Erdinç MERMER* and Prof. Dr. Serkan ÖZGEN**

*TÜBİTAK Space Technologies Research Institute

Ankara Turkey

**Middle East Technical University

Ankara Turkey

Abstract

The aim of the study is to design a HALE UAV using both turbofan engine and solar energy in order to obtain at least 24 hours endurance with 250 kg camera and 750 kg battery total 1000 kg payload capacity and 6096m (20000 ft) to 9144 m (30000 ft) service ceiling. During daytime, required power is obtained from solar panels. Morover, excess solar energy is used for charging the lithium-ion battery. It is assumed that turbofan engine is used only for climbing to the required altitude. During loiter, only solar energy and battery power are used. The design methodology consists of two main parts. In the first part, typical conceptual design methodology is used. Weight analysis, wing loading and thrust loading, required power analysis, aircraft performance analysis are performed. While performing the conceptual design, aircraft is assumed as a turbofan-powered aircraft. Due to long wingspan and large wing area, typical structural weight determination techniques are not suitable for the HALE UAV. Therefore, a new structural weight prediction model is used. In the second part of the thesis, solar energy and battery energy are examined in order to assess whether endurance and service ceiling requirements are satisfied. Solar radiation model is used for verification.

1. Introduction

Solar powered aircraft systems have been studied approximately since 40 years. Solar cell technology has been developed in terms of cell efficiency since many years, which is promising for solar-based aircraft concepts when compared to conventional long endurance aircraft. The most recent solar-based aircraft are the Solar Impulse and Qinetiq Zephyr systems, which are using solar cells with efficiency of 22% and 28%, respectively. Moreover, GaAs-based solar cells with around 30% efficiency are commonly used in space industry and this technology has almost exceeded 40% of efficiency recently. Although the cost of this technology is high at the moment, the use of GaAs-based solar cells in airborne and spaceborne missions in the near future will be commonplace, decreasing the cost for affordable missions. Due to the fact that the solar radiation is available only during daytime, the battery is the only source of power during night flight. Solar Impulse is one of the most important competitors for this study because of its advanced battery technology. Solar impulse obtains its nighttime energy from 4 pieces of 164 kWh/kg Li-Ion batteries, while Qinetic Zephyr uses 350 kWh/kg Lithium Sulphur batteries. In the near future, Sulphur based batteries will be used more commonly for solar powered aircraft since their energy density is nearly as twice as much as ion based ones.

1.1 Conceptual Design

Before starting the conceptual design, it is essential for designers to remember that most of the airplane designs are evolutionary, not revolutionary. Therefore, choosing suitable competitor aircraft and specifying applicable requirements is very important. The conceptual design begins with requirements. Hybrid UAV design requirements for the current study are stated in Table 1.

Table 1 Requirements

Payload (kg)	Endurance (hour)	Range (nm)	Cruise Speed (m/s)	Service Ceiling (km)	Stall Speed @ sea level (m/s)
1000	24-48	1000	35	9-21	50

The competitor study is performed to predict the aircraft initial geometric and weight parameters, for instance, aspect ratio and weight fractions. From the competitor study, average empty weight fraction is found as 0.6218, aspect ratio is found as 24.5. $L/D)_{max}$ is assumed as 40, average wingspan is calculated as 66.45 m and average chord length is calculated as 2.44 m. Since there are no hybrid aircraft design data in the literature, competitor aircraft have been chosen among HALE UAVs and solar powered UAVs, as shown in Table 2.

Table 2 Competitor Aircraft

Aircraft	Phantom Eye 2010	Global Observer 2 2005	Global Hawk 1998	Lockheed U2S 2010	Condor 1989
Length	16 m	25 m	14 m	22.4 m	19.2 m
Wingspan	65 m	79 m	35 m	71.9 m	31.4 m
Empty Weight	3700 kg	2750 kg	3851 kg	2300 kg	14300 kg
Gross Weight	4561 kg	4168 kg	10387 kg	2300 kg	18500 kg
Propulsion	Hydrogen	Hydrogen	Turbofan	Turbofan	Turboprop
Thrust/Power	2x112 kW	-	31 kN	86 kN	130 kW
Range	13000 km	17300 km	24985 km	1541 km	--
Endurance	7 days	7 days	36 hours	12 hours	80 hours
Service Ceiling	20 km	20 km	20 km	12 km	21.3 km

1.2 Mission Profile

Simple cruise and loitering mission profile is sketched in Figure *1*; Segment 0-1 indicates the engine start, taxi and takeoff, segment 1-2 represents climb, phase 2-3 represents cruise, segment 3-4 represent loiter, segment 4-5 represents cruise back, segment 5-6 represents descent, and segment 6-7 represents landing and stop.
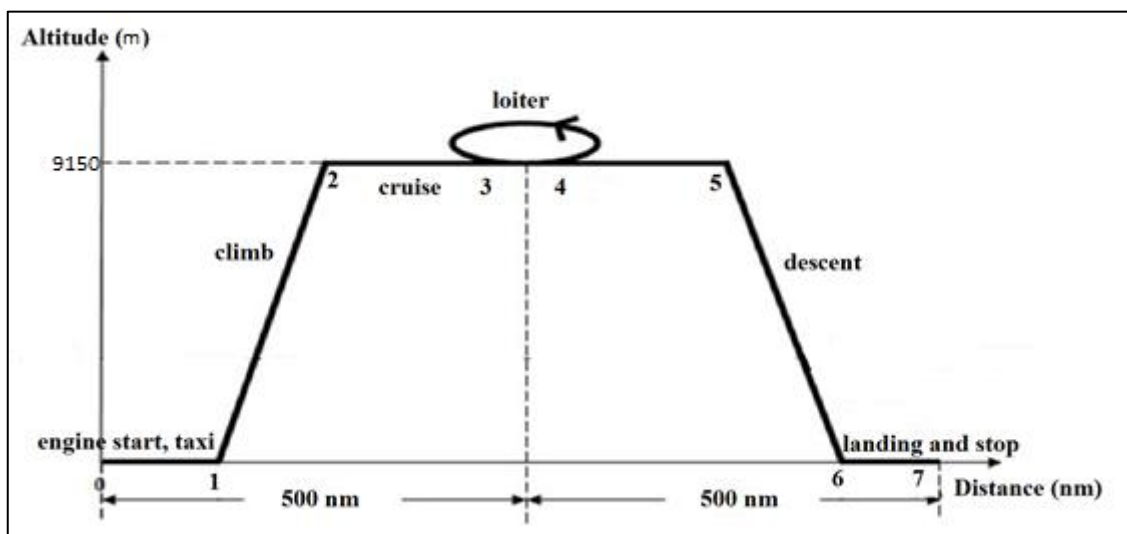

Figure 1 Mission Profile

Mermer, Özgen

Takeoff gross weight is the total aircraft weight including crew, payload, empty and fuel weights.

$$W_0 = W_{crew} + W_{payload} + W_{fuel} + W_{empty} \tag{1}$$

While estimating takeoff gross weight Table 2 [1] is used. Constants which are for high altitude UAV are used for calculations. $A = 2.75, c = -0.18$ and $K_{vs} = 1$ for fixed sweep wing.

Fuel weight depends on the mission to be flown, the fuel consumption rate of the engine and aerodynamics of the aircraft. As indicated in Figure *1*, mission profile is separated into 7 parts. Each phase of the mission is represented by a weight fraction. At the end of the mission, all weight fractions are multiplied and fuel weight fraction is calculated. For a simple cruise mission Raymer [1] describes fuel weight and gross weight calculations as follows:

$$W_f = W_0 - W_7 \tag{2}$$

Where W_f represents the fuel weight of the aircraft, W_0 symbolizes the takeoff gross weight of the aircraft and W_7 stands for the weight of the aircraft at the end of the mission. It is assumed that the fuel tanks are completely empty at the end of the flight except for trapped and unused fuel, see below. The weight fractions for each phase is calculated as follows.

(0-1) For the engine start, taxi and takeoff, historical trend is used [1]:

$$\frac{W_1}{W_0} = 0.97 \tag{3}$$

W_0 is the takeoff weight of the aircraft.

(1-2) For climb, historical trend is used [1]:

$$\frac{W_2}{W_1} = 0.985 \tag{4}$$

Where W_2 is the weight of the aircraft at the beginning of cruise.

(2-3) For cruise, Breguet range equation is used [1]:

$$\frac{W_3}{W_2} = \exp\left(\frac{-Rc_t}{V(L/D)}\right) = 0.9759 \tag{5}$$

where W_3 is the weight of the aircraft at end of the cruise and $(L/D)_{cruise} = 0.866 * (L/D)_{max}$ and specific fuel consumption is taken as $c_t = 0.4/h$.

(4-5) Cruise back:

$$\frac{W_5}{W_4} = \frac{W_3}{W_2} \tag{6}$$

where W_4 is the weight of the aircraft at end of the loiter and W_5 is the weight of the aircraft at end of the cruise back.

(5-6) For descent, historical trend is used [1]:

$$\frac{W_6}{W_5} = 0.992 \tag{7}$$

W_6 is the landing weight of the aircraft.

(6-7) For landing and stop, historical trend is used [1]:

$$\frac{W_7}{W_6} = 0.993 \tag{8}$$

As a result:

$$\frac{W_7}{W_0} = \frac{W_7}{W_6}\frac{W_6}{W_5}\frac{W_5}{W_4}\frac{W_4}{W_3}\frac{W_3}{W_2}\frac{W_2}{W_1}\frac{W_1}{W_0} = 0.7896 \tag{9}$$

$$\frac{W_f}{W_0} = 1.06\left(1 - \frac{W_7}{W_0}\right) = 0.223 \tag{10}$$

assuming that 6% is the reserve or trapped fuel. Using the takeoff gross weight estimation equation:

$$W_0 = \frac{W_{payload}}{1 - 2.75(W_O)^{-0.18} - \frac{W_f}{W_0}} \qquad (11)$$

Takeoff gross weight and fuel weight is calculated as:

$$W_0 = 4105 \ kg \ \ and \ W_f = 914.5 \ kg$$

By assigning service ceiling as 9150 m (30000 ft) and range as 1000 nm, take off gross weight is determined iteratively using equation 11.

After determining the takeoff gross weight, thrust to weight ratio calculations are performed. Calculations are done by using 5 desired performance parameters. While determining T/W, an initial wing loading is assumed, which is assigned as 24.45 kg/m^2 based on competitor study, yielding T/W = 0.175. Aspect ratio is calculated using competitor average aspect ratio, which is 24.5.
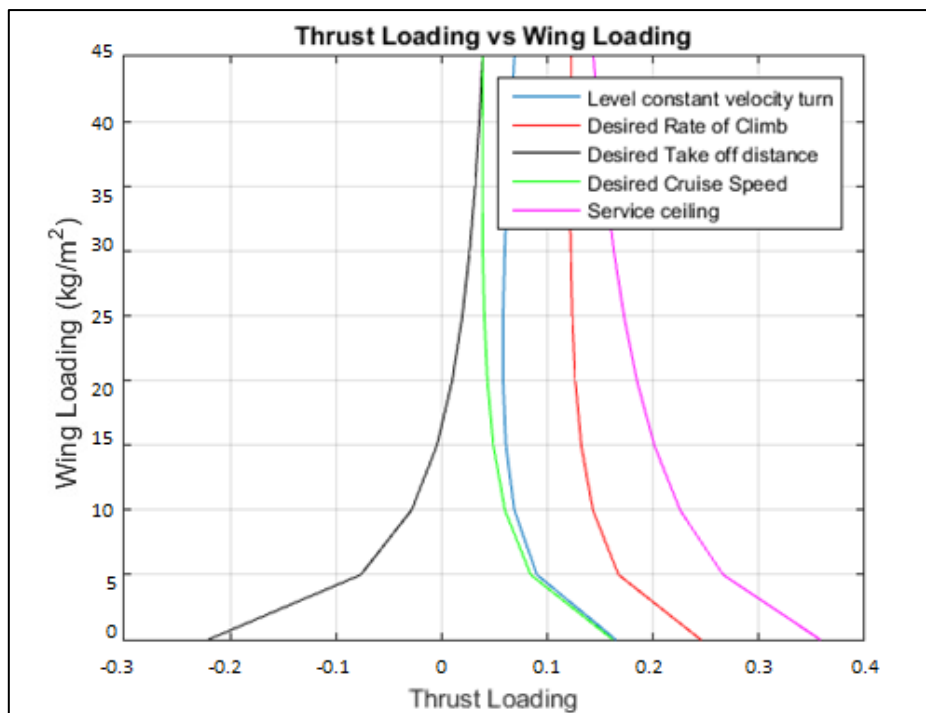

Figure 2 Thrust Loading vs. Wing Loading

Wing loading is another crucial parameter for aircraft design since almost all performance characteristics depend on wing loading. Optimum wing loading is calculated by using aircraft design requirements such as takeoff distance, landing distance, cruise speed, stall speed, instantaneous turn and sustained turn. The lowest wing loading is chosen after calculations since the lowest wing loading, i.e. largest wing satisfies all of the requirements. Wing loading calculations are performed with various velocity values, because observing the effects of the velocity changes on wing loading is useful when surveying performance parameters at different altitudes. After all calculations, the lowest wing loading becomes W/S = 24.9 kg/m^2 corresponding to the cruise velocity wing loading. Wing area can be determined by dividing the weight estimation by wing loading. The results of this calculation yields the wing planform area as 165 m^2.

Using the aspect ratio and planform area, wingspan can be calculated from equation 12 as 63.55 m

$$AR = \frac{b^2}{S} \qquad (12)$$

Up to now, aspect ratio, wingspan and wing area are determined. As known, elliptic lift distribution is very important for long wingspans since they are prone to structural failure due to high bending moments at the root. Generally, solar airplanes which have long wingspan, have variable taper ratio in order to obtain elliptic lift distribution. Also,

this provides more wing area for solar cell placement. Taper ratio of 1 is better for solar panel placement. On the other hand, taper ratio of 0.5 is more convenient for attaining elliptic lift distribution on wing. Therefore, taper ratio between 0.5 and 1 is a good compromise. Using values founded above wing geometry is constructed in XFLR5 [17], as shown in *Figure* 3. Taper ratio was calculated as 0.721. Mean chord length is calculated as 2.68 m. Spanwise location of the mean chord is calculated as 15.04 m. Raymer [1] wing geometry calculation methods are used for calculations:

$$C_{root,wing} = \frac{2S}{b(1 + \lambda)} = \frac{2 \times 165}{63.55(1 + 0.721)} = 3.22 \ m \qquad (13)$$

$$C_{tip,wing} = \lambda C_{root,wing} = 1.58 \ m \qquad (14)$$

$$\bar{y} = \frac{b}{6}\left(\frac{1 + 2\lambda}{1 + \lambda}\right) = 15.03 \ m \qquad (15)$$

$$\bar{c}_{wing} = \frac{2}{3} C_{root,wing} \frac{1 + \lambda + \lambda^2}{1 + \lambda} = 2.68 \ m \qquad (16)$$

Figure 3 Details of wing geometry

T-tail configuration is chosen as the tail configuration because this allows more surface on the horizontal tail that can be used for the solar panels. Horizontal tail area can be determined from the equation 17.

$$S_{HT} = \frac{c_{HT} \bar{C}_W S_W}{L_{HT}} \qquad (17)$$

c_{HT} is the volume coefficient of the horizontal tail. Using volume coefficients of the competitor aircraft is convenient and are indicated in Table 3 Coefficients of Intelligence, Surveillance and Reconnaissance (ISR) aircraft are used for calculations.

Table 3 Tail volume coefficients of competitor aircraft [2]

Aircraft	Horizontal tail volume coefficient	Vertical tail volume coefficient
Lockheed Martin U-2S	0.34	0.014
Northrop Global Hawk	0.32	0.0186
Boeing Condor	0.53	0.012
ISR	0.34	0.014

Horizontal tail area is thus calculated as 15 m^2. Aspect ratio of the horizontal tail is taken as 8 as indicated in Table 4.3 of reference [1]. Using Equation 18, vertical tail area is determined as 14.5 m^2.

$$S_{VT} = \frac{c_{VT} b_W S_W}{L_{VT}} \qquad (18)$$

After all calculations are performed aircraft geometry is determined which is presented in Figures 4, 5 and 6.
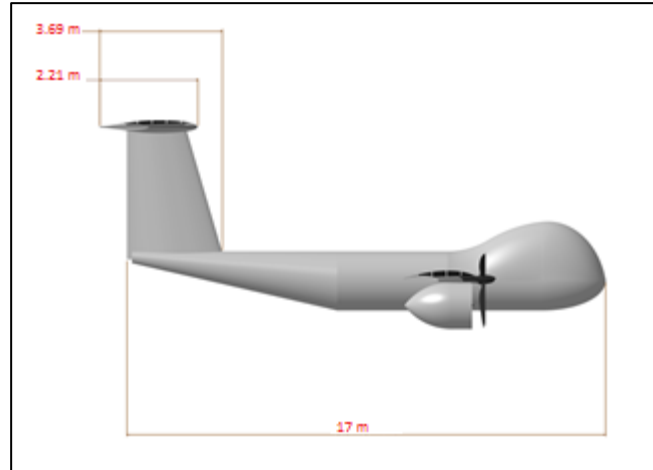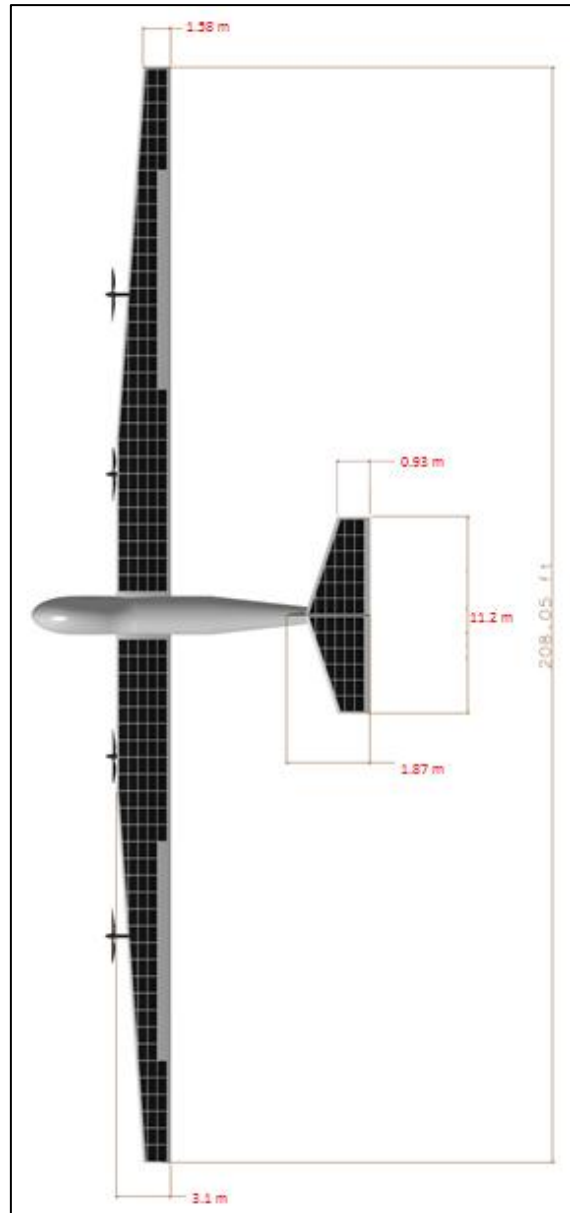
Figure 4 Side view of the aircraft

Figure 5 Top view of the aircraft

Figure 6 Isometric view of the aircraft

After geometry determination, drag calculations were performed. Subsonic parasite drag coefficient can be estimated by using the component build-up method and its equation is given below [1]:

$$C_{D_0} = \frac{\sum C_{fc} \, FF_C \, Q_c \, S_{wet,c}}{S_{ref}} + C_{D_{misc}} + C_{D_{L\&P}} \qquad (11)$$

where:

C_f: Skin friction factor
FF: Form factor (shape factor)
Q: Interference factor
$C_{D_{misc}}$: Miscellaneous drag
$C_{D_{L\&P}}$: Leakages and protuberances drag

In order to calculate skin friction coefficient, C_f, Reynolds number should be found in order to determine whether the flow is laminar or turbulent. If the Reynolds number is greater than 1000000, flow is fully turbulent and skin friction coefficient for fully turbulent flow can be used:

$$C_f = \frac{0.455}{(logRe)^{2.38}(1 + 0.144M)^{0.65}} \qquad (20)$$

Drag calculations were done for sea level, 20000 ft and 45000 ft altitude. Landing gear parasite drag coefficient is taken into account at sea level.

Table 4 $C_{D,0}$ at Sea Level

Sea Level	Re	C_f	FF	$C_{D,0}$
Wing	5.13E+06	0.0033	1.11	0.008600
Fuselage	2.84E+07	0.0026	1.21	0.000245
Vertical Tail	5.03E+06	0.0034	1.10	0.000625
Horizontal Tail	2.42E+06	0.0038	1.10	0.000913
Total zero lift drag coefficient				0.0129

Table 5 $C_{D,0}$ at 6096 m (20000 ft) altitude

20000ft	Re	C_f	FF	$C_{D,0}$
Wing	3.07E+06	0.0037	1.11	0.001900
Fuselage	1.70E+07	0.0028	1.21	0.001046
Vertical Tail	3.02E+06	0.0037	1.10	0.000718
Horizontal Tail	1.45E+06	0.0042	1.10	0.009736
Total zero lift drag coefficient				0.0134

Table 6 $C_{D,0}$ at 13716 m (45000 ft) altitude

45000ft	Re	C_f	FF	$C_{D,0}$
Wing	1.25E+06	0.0043	1.12	0.01146
Fuselage	6.95E+06	0.0032	1.21	0.00084
Vertical Tail	1.23E+06	0.0043	1.10	0.00123
Horizontal Tail	5.96E+05	0.0049	1.10	0.00217
Total zero lift drag coefficient				0.0157

1.3 Required Power and Velocity Calculations

During loiter, airplane uses solar energy and battery energy so power required curve is needed in order to find the minimum power needed and the optimum flight velocity. As can be seen in *Figure* 7, at 6096 m altitude, minimum power required for loiter is 32.73 kW, and the optimum velocity for loiter is 24.4 m/s. At 9144 m altitude, minimum power required for loiter is 39.19 kW and the optimum velocity for loiter is 27.43 m/s. At 13716 m altitude, minimum power required for loiter is 53.88 kW, and the optimum velocity for loiter is 36.58 m/s. 10% excess power was added to the calculations to account for the power requirement of avionics and payload. Available solar power and battery power are calculated later.
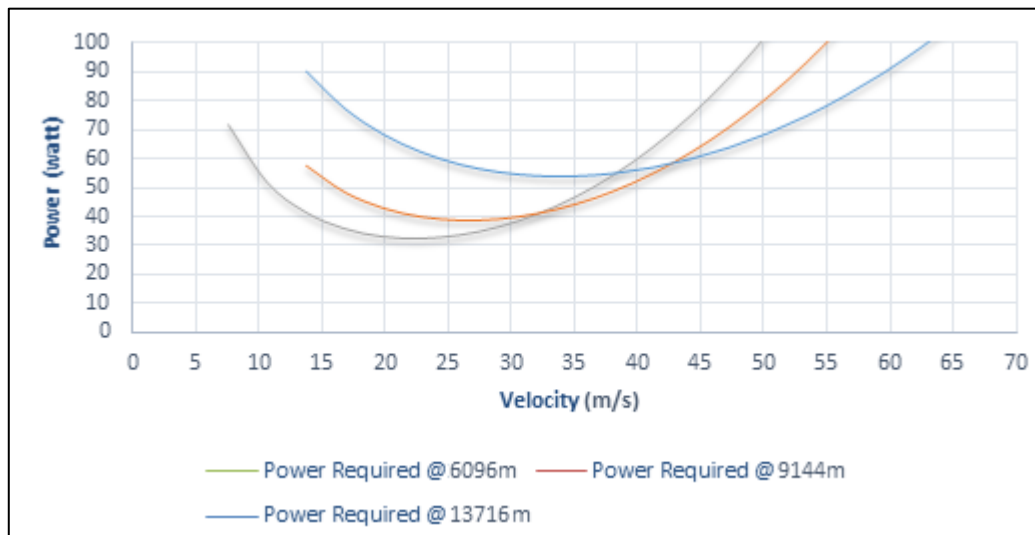

Figure 7 Power required vs Velocity

In this part, energy required and energy available diagrams are drawn using real time simulations. Energy balance diagram shows the power needed for flight, solar irradiance and battery power. Main aim is to obtain 48 hours of endurance or more. By defining payload weight main aim is to carry about 250 kg payload, the remaining 750 kg belonging to the battery. Total solar panel area is taken as 150 m^2. It is assumed that usable wing area for solar

panels is 140 m². Solar panels are not used on the regions on the wing which have high curvature and the control surfaces. Also using same assumptions, solar panel area on horizontal tail is estimated as 10 m^2.

1.4 Solar Irradiance

Duffie J. A., Beckman W. A. [32] solar irradiance model is used for illustrating daily solar energy obtained. Model is based on day number (1 January represents 1, 31 December represents 365), pressure, solar irradiance constant, and latitude. Location of city of Ankara is used for simulating endurance.

Table 7 Representation of Solar Irradiance Constant

Constant	Representation
d	Day of the year
ϕ	Latitude
P	Pressure
h	Hour
G_{sc}	Radiation constant
P_0	Pressure at sea level
g	The acceleration of gravity
δ	Declination
τ	Atmospheric transmittance for beam radiation
v	Extraterrestrial radiation

$$v^2 = \left(1 + 0.033 \times cos\frac{360 \times d}{365}\right) \tag{21}$$

$$\delta = 23.45 \times sin\left(\frac{360 \times (284 + d)}{365}\right) \tag{22}$$

$$P_s = G_{sc} \times A_s \times v^2 \times (sin\delta \times sin\phi + cos\left((h - 12) \times 15\right) \times cos\delta \times cos\phi) \tag{23}$$

$$\tau = \frac{p}{p_0} \times (\sqrt{1229 + (614 \times cos(\phi - \delta))^2} - 614 \times cos(\phi - \delta)) \tag{24}$$

$$A_s = 0.5 \times (e^{-0.65 \times \tau} + e^{-0.095 \times \tau}) \tag{25}$$

A_s represents the solar radiation per area. If all calculations are made for 21 June Ankara namely 40° North, solar irradiance graph shown in Figure 8 is obtained.
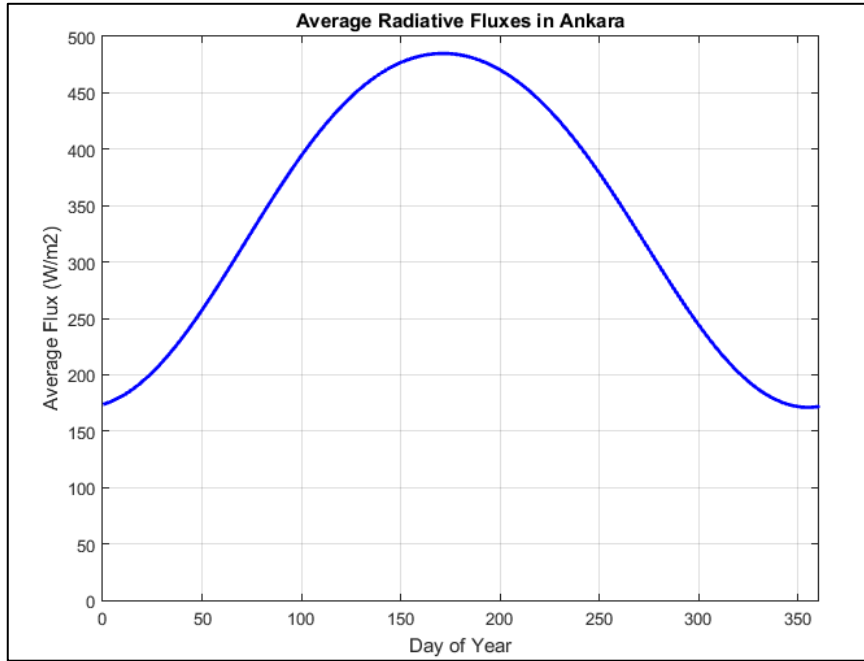
Figure 8 Average Annual Solar Radiation Fluxes of Ankara

Area under the curve gives the total solar energy. In Ankara sun rises at 4.50 am and sets at 19.50 pm on June 21 as seen from *Figure* 9. Radiation flux of June 21 is approximately 3 times higher than radiation flux of 21 December as can be seen from Figure 8. Therefore, it is expected that endurance reduces dramatically in winter for solar powered aircraft.
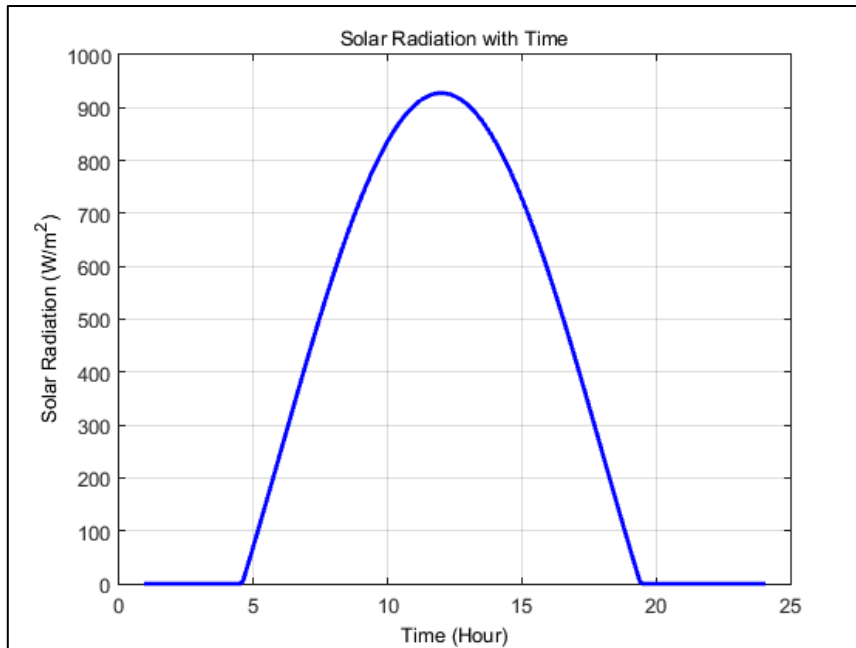

Figure 9 Solar Radiation of Ankara on June 21

1.5 Solar Energy Calculation

Total energy gained from solar radiation is calculated from equation 26:

$$E_{elec,tot} = \frac{I_{max} \times T_{day}}{\pi/2} \times A_s \eta_{wthr} \eta_{sc} \eta_{cbr} \eta_{mppt} \tag{26}$$

where:

η_{wthr} is the weather efficiency, namely if there is a clear sky or dark sky. It is assumed that the sky is clear.

η_{sc} is the solar cell efficiency taken as 0.3.

η_{cbr} is the wing camber efficiency taken as 0.9. It is calculated by using wing upper surface slope. It ıs calculated by taking both oncoming airfoil upper surface coordinate data and calculating its slope. Solar panels are not used on area having high slope.

η_{mppt} (Sunlight conversion system efficiency) is taken as 0.95.

The efficiency values are summarized in Table 8.

Table 8 Efficiency of Solar Instruments

Instruments	Efficiency
Cell configuration	0.93%
MPPT	0.97%
MPPT tracking	0.95%
Charge/Discharge	0.986%
Propeller	0.8%
Electric Motor	87%
Gearbox	95%

Required energy is calculated before conceptual design phase. Power required analysis is performed in order to simulate loitering phase. During simulation, the flight efficiencies are assumed as constant. Also, it is assumed that aircraft flies in clear sky. Wind is assumed as steady, there is no gust. During simulations, batteries are taken as fully charged before takeoff.

Battery is one of the most important components for solar powered aircraft. When determining battery properties, Solar Impulse's battery technology is used, since Solar Impulse designers use the most cost and energy efficient batteries. Moreover battery availability is another crucial parameter for designers. Therefore, if one who wants to design a solar powered aircraft, must take into account the availability of technological instruments. Specific energy of the Solar Impulse's batteries is greater than 259.45 Wh/kg, which means they are efficient enough and available for Hybrid UAV. There are 4 pieces of 41 kWh lithium-ion batteries and total 52 kW power plant on Solar Impulse. Each battery weighs 157.85 kg and 5 identical batteries are used for this study. Also, it is assumed that excess solar energy is stored in the batteries. Battery charge and discharge efficiencies are taken as 0.986 [4].

1.6 Real Time Simulation

Theory of real time simulation is based on energy balance of the system. Aircraft takes off with fully charged batteries. Until flying up to the mission area and altitude, turbofan engine is used. Then solar irradiance energy and battery energy are used. If required power becomes greater than the available power, simulation stops. Optimum takeoff time is found by trying different times of the day. For instance, On June 21 maximum endurance occurs when aircraft starts loitering at 24.00. On the other hand, On December 21 (shortest daytime) maximum endurance time occurs when aircraft starts loitering at 06.00 am. Simulations are performed for 2 additional different days of the year which are 21 March, 23 September. Solar radiation on equinoxes are same. Differences are sunrise and sunset times. Simulations are performed for each day in order to show the optimum loitering hours.

1.7 Methods for Reconstructing Solar Cycle

Major advantage of the hybrid system is the possibility of reconstructing the solar cycle. One way is to add excess fuel to the aircraft in order to attain to the point where required power is equal to the solar power obtained from solar panels. After reaching that point, cycle restarts.

Another method is the unpowered gliding method. In other words, if required energy becomes more than available solar and battery energy, aircraft starts unpowered gliding in order attain to the point where required power is equal to the solar power obtained from solar panels. For instance when aircraft loiters at 13716 kg with 40% efficient solar

cells on June 21, approximately 4 hours are needed to reach to that point. After 4 hours of unpowered gliding, solar cycle restarts at 1524 m altitude at 11.00 am.

2. Simulations of Various Cases

First case is the lowest altitude case. At 6096 m aircraft needs 32 kW power in order to sustain loitering. As mentioned before, 4 different days of the year are used for illustrating loitering time.

2.1 Simulations for 30% Efficient Solar Cells

2.1.1 6096 m, June 21, 30% Efficient Solar Cells

The longest daytime of the year in the northern hemisphere occurs on 21 June. Sun rises at 04:50 am. Aircraft starts loitering at 24:00. All simulations are performed for location of Ankara (40° latitude).

As mentioned before, when required power is less than battery power and solar powered gained from sun, simulation stops. For this case, simulation stops after 21.3 hours loitering as can be seen in Figure *10*. Reconstruction method suggests that, firstly, the time between simulation stops (A) and the point, where the power gained from sun is equal to the required power (B), is calculated. There are 9.5 hours between point (A) and point (B), Figure *11*.
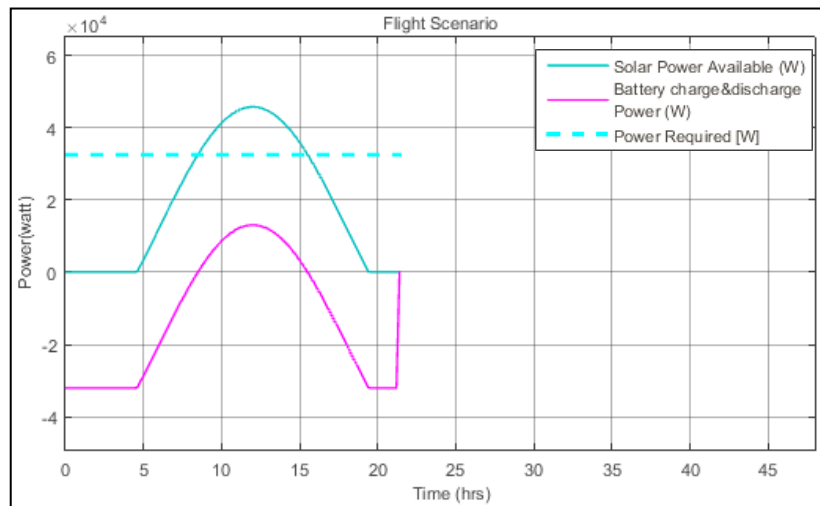

Figure 10 Energy Balance Diagram with 30% efficient solar cells on June 21
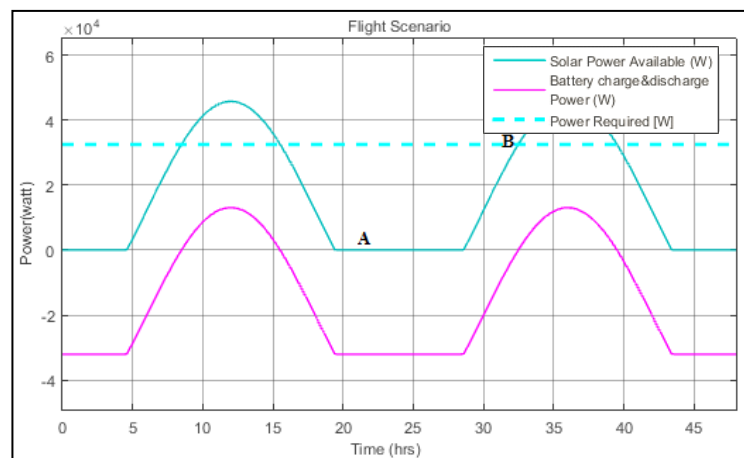

Figure 11 Required Time Calculation for Reconstructing Solar Cycle with 30% Efficient Solar Cells on June 21

9.5 hours loitering flight must be sustained by the turbofan engine in order to reconstruct the solar cycle. Secondly, weight estimation equation is used in order to find required fuel by assuming that aircraft flies only by turbofan. Weights are estimated again with iteration method as calculated before. Using equations 2 to 12

$\frac{W_1}{W_0} = 0.97$, engine start, taxi and takeoff, historical trend was used.

$\frac{W_2}{W_1} = 1.0065 - 0.325M^2$,

$\frac{W_3}{W_2} = \exp\left(\frac{-Rc_t}{V(L/D)}\right)$, then $exp\left(\frac{-6076100 \times 1.11 \times 10^{-4}}{2 \times 110 \times (35)}\right) = 0.9228$.

Specific fuel consumption was taken as 0.4/h.

$$Endurance = \exp\left(-\frac{Ec_t}{L/D}\right) \tag{27}$$

$\frac{W_4}{W_3} = e^{\frac{Ec_t}{L/D}} = 0.8971$, where endurance is 9.5 hours.

$\frac{W_5}{W_4} = \frac{W_3}{W_2}$, cruise back,

$\frac{W_6}{W_5} = 0.992$, descend,

$\frac{W_7}{W_6} = 0.993$, landing and stop.

$$\frac{W_7}{W_0} = \frac{W_7}{W_6}\frac{W_6}{W_5}\frac{W_5}{W_4}\frac{W_4}{W_3}\frac{W_3}{W_2}\frac{W_2}{W_1}\frac{W_1}{W_0} = 0.7387,$$

$$\frac{W_f}{W_0} = 1.06\left(1 - \frac{W_7}{W_0}\right) = 0.277$$

Also, $\frac{W_4}{W_0} = \frac{W_4}{W_3}\frac{W_3}{W_2}\frac{W_2}{W_1}\frac{W_1}{W_0} = 0.789$. Hence, W_0 is calculated from:

$$W_0 = \frac{W_{payload}}{1 - 2.75(W_O)^{-0.18} - \frac{W_f}{W_0}}$$

After iterations, $W_o = 5450$ kg is calculated. Then W_4 is calculated as 4295 kg. Therefore:

$\frac{W_3}{W_0} = \frac{W_3}{W_2}\frac{W_2}{W_1}\frac{W_1}{W_0} = 0.88$, and $W_3 = 4780\ kg$, during 9.5 hours loiter and $4780 - 4295 = 485$ kg fuel is consumed.

If 595 kg. excess fuel added to the fuel tanks before takeoff, solar cycle can be reconstructed and endurance becomes 48 hours. But it is too heavy for aircraft to fill in such an excess fuel before takeoff. Therefore optimizing excess fuel method does not work for these conditions.

2.1.2 6096 m, March 21, 30% Efficient Solar Cells

With same conditions except the day of the year, simulations are performed and following results are obtained. Sun rises at 05:50 am and the maximum endurance occurs when aircraft starts loitering at 05:50 am. Loitering lasts 17.1 hours.
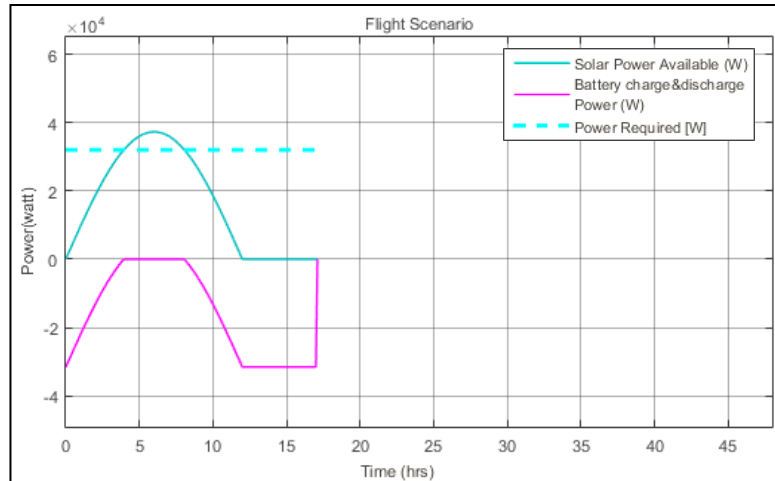
Figure 12 Energy Balance Diagram with 30% Efficient Solar Cells on March 21

As seen from Figure *12*, loitering endurance is 17.2 hours. Time needed for reconstructing the solar cycle is 10.2 hours, *Figure* 13. Using equations 2 to 12 excess fuel is calculated as 548 kg. It does not make sense to reconstruct solar cycle for these conditions.
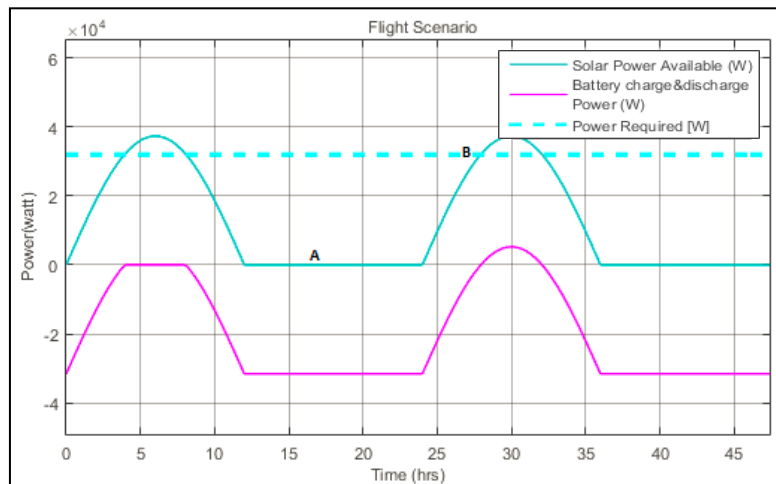

Figure 13 Required Time Calculation for Reconstructing Solar Cycle with 30% Efficient Solar Cells on March 21

2.1.3 6096 m, September 23, 30% efficient solar cells

23 September flight conditions give approximately same results with 21 March as seen from *Figure* 14. Airplane starts loitering at 04:00 am.
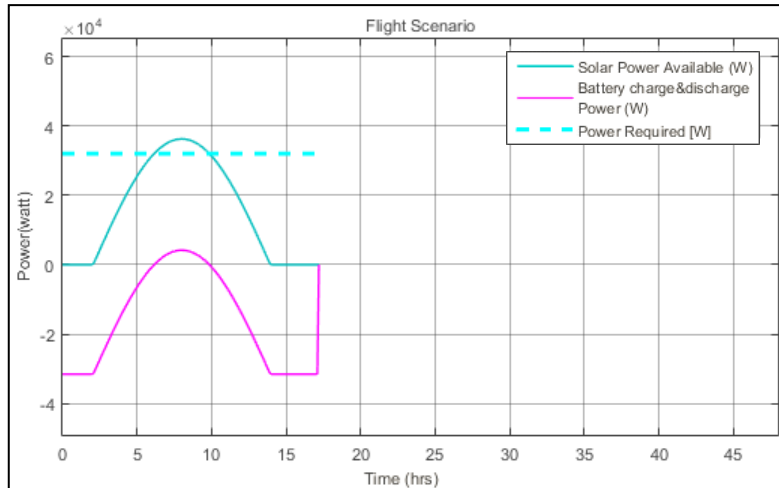
Figure 14 Energy Balance Diagram with 30% Efficient Solar Cells on September 23

2.1.4 6096 m, December 21, 30% Efficient Solar Cells

On December 21, namely shortest daytime in the year, hybrid airplane endurance time is relatively short due to less solar irradiance. Endurance is approximately 12.3 hours when aircraft starts loitering at 07:00 am, *Figure* 15. Available power never becomes equal to the required power. Therefore, optimizing excess fuel method does not work.
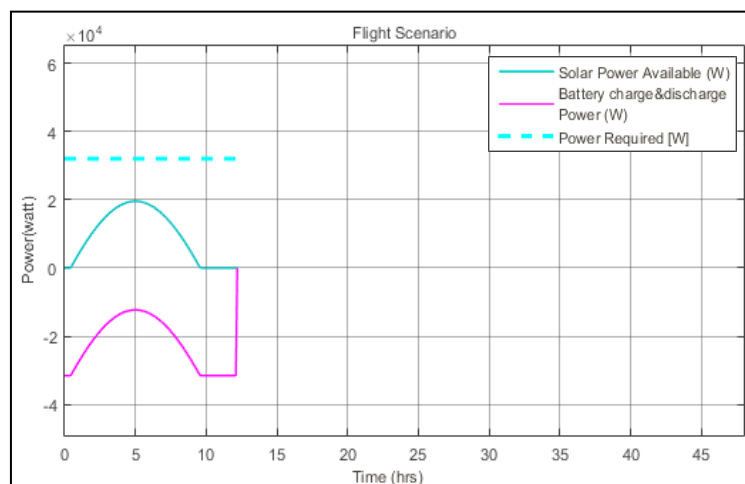

Figure 15 Energy Balance Diagram with 30% Efficient Solar Cells at December 21

2.2 Simulations for 40% Efficient Solar Cells

After 30% efficient solar cells simulations, it is observed that 40% efficient solar cells are more suitable for the current design. As mentioned before, these solar cells are really expensive for solar aircraft. Currently, solar powered aircraft use 22% efficient solar cells. Developments state that 10 years later 40% efficient solar cells might be feasible for solar powered aircraft technology. Following simulations are done by using 40% efficient solar cells.

2.2.1 6096 m, June 21, 40% Efficient Solar Cells

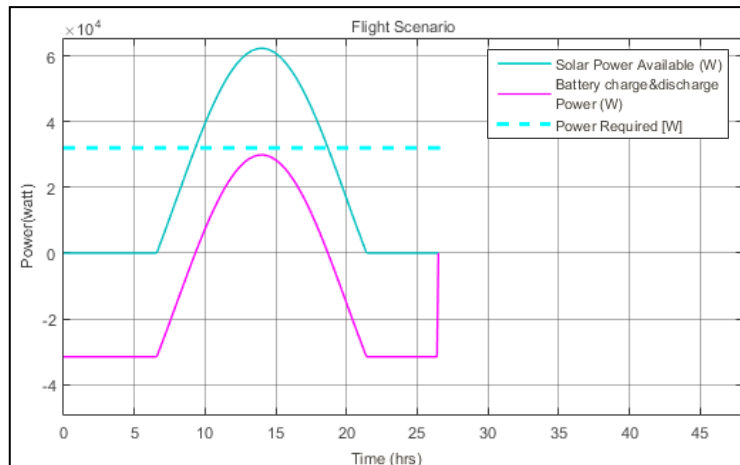As seen from Figure *16* maximum endurance becomes 26.6 hours when aircraft starts loitering at 22:00 pm.

Figure 16 Energy Balance Diagram with 40% Efficient Solar Cells on June 21

There are 5.5 hours between the times when the simulation ends (A) and solar power available which is equal to the power required (B) as can be seen in Figure *17*.
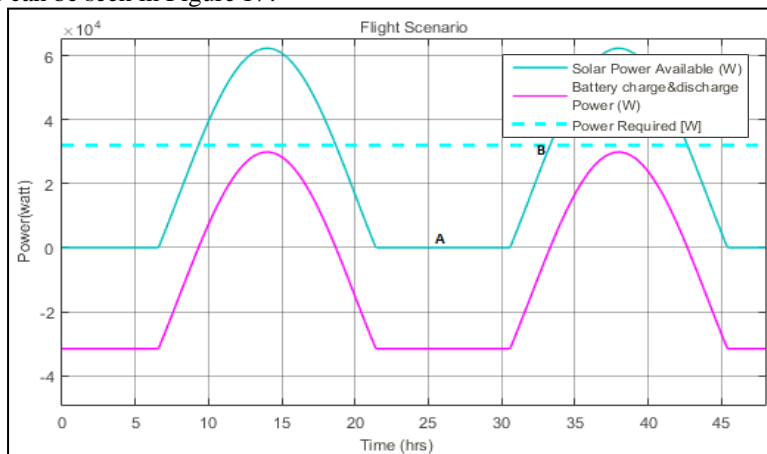

Figure 17 Required Time Calculation for Reconstructing Solar Cycle with 40% Efficient Solar Cells on June 21

Time needed for reconstructing the solar cycle is 5.5 hours. Using Weight equations 2 to 12 and gross weight calculated as 4817 kg, $W_3 = 4240\ kg$ and $W_4 = 4087\ kg$. During 5.5 hours loiter, $4240 - 4087 = 153\ kg$ fuel is consumed. If 153 kg excess fuel is added to the fuel tanks before takeoff, solar cycle can be reconstructed and endurance becomes 67 hours.

2.2.2 6096 m, March 21, 40% Efficient Solar Cells

As seen from Figure *18* loiter endurance is calculated as 20.6 hours when aircraft starts loitering at 23:00. There are 6.25 hours between the time when the simulation ends (A) and solar power available which is equal to the power required (B) as illustrated in Figure *19*.
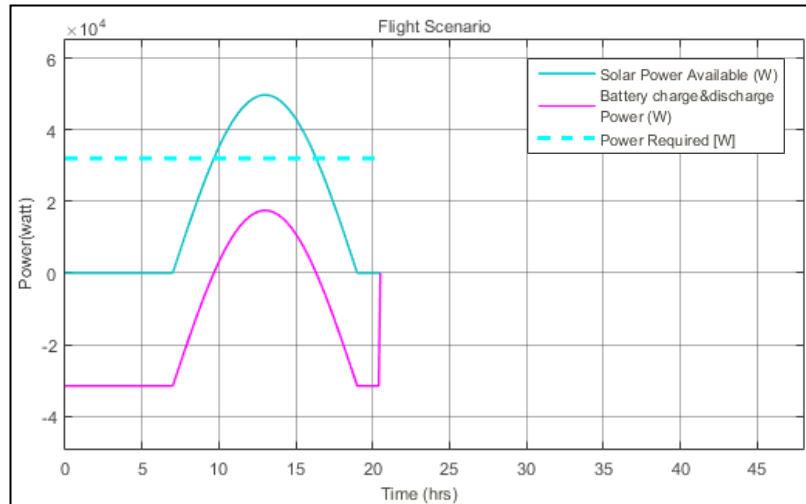
Figure 18 Energy Balance Diagram with 40% Efficient Solar Cells on March 21
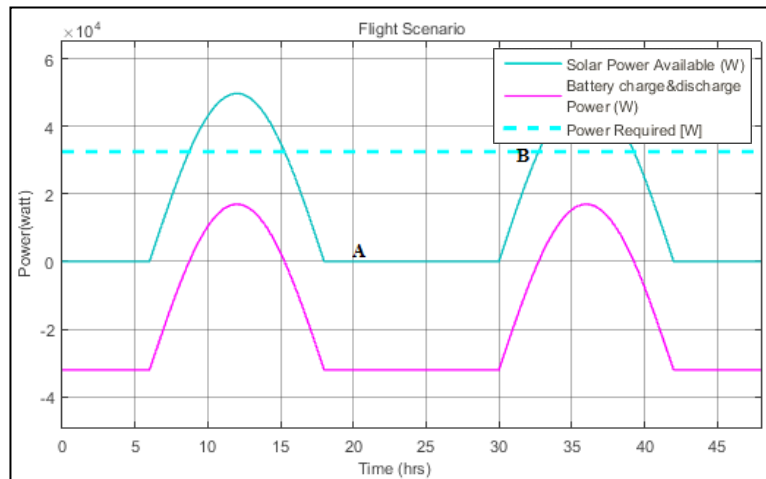

Figure 19 Required Time Calculation for Reconstructing Solar Cycle with 40% Efficient Solar Cells on March 21

Time needed for reconstructing the solar cycle is 13 hours. Using Weight equations 2 to 12 , gross weight is calculated as 5774 kg, W_3 is calculated as 5081 kg and W_4 is calculated as 4462 kg. During 13 hours loiter, $5081 - 4462 = 619 \ kg$ fuel is consumed. If 619 kg excess fuel is added to the tanks before takeoff, solar cycle can be reconstructed, which is not very meaningful because it is too heavy to be used for current design.

3. Conclusions

This study is a combination of the conceptual design of a turbine engine HALE UAV and a solar powered UAV. Within this aspect, this study is unique. Conventional conceptual designs of UAVs having turbine engines do not work for HALE UAV designs, because high aspect ratio and large wing area lead to wrong weight and performance estimations. Therefore, new design principles must be developed especially about prediction of weight and performance equations, which include the aspect ratio term. Hence, some assumptions are made while predicting wing weight and span efficiency factor. Also when estimating gross weight, batteries are assumed as payload.

The second part of the study is about loitering performance. Loitering performance is simulated for 4 different days of the year, (21 March, 21 June, 23 September and 21 December) for 2 different solar cell efficiencies (30% and 40%) and 6096 m altitude. As a result, the longest endurance occurred with 40% efficient solar cells, at 6096 mt altitude and on 21 June when the solar irradiance is maximum. After simulations, it is seen that maximum endurance is 27.4 hours without excess fuel. Main aim of the project is to attain 48 hours loitering endurance. Therefore, a

method called excess fuel calculation is used. Filling excess fuel to aircraft before takeoff is the best option in order to reconstruct the solar cycle and reach minimum 48 hour loitering endurance. Method suggests that excess fuel, calculated using weight prediction model, can be used for predicting the fuel in order to find the fuel consumed for reaching the point where required power is equal to the solar power available obtained from solar cells. After excess fuel method is performed, it is observed that this method is suitable only when aircraft flies on June 21, at 6096 m with 40% efficient solar cells. After the solar cycle is reconstructed, Aircraft reaches 67 hour endurance.

Main drawbacks of solar HALE UAV with higher payloads are inadequate climb rates and very limited maximum speed. It may take a long time for reaching the desired target area or fly away from it. Hybrid UAV satisfies relatively high maximum speed and rate of climb thanks to its turbofan engines.

Continuous flight of solar airplanes depend mainly on the sunlight. Endurance reduces dramatically during winter since, nights are longer and available sunlight is limited. Because of that reason, solar aircraft projects and studies are tested during summertime. Sun angle is another crucial parameter for available solar power calculations. Sun angle must be taken into account during calculations. Solar irradiance equation includes the latitude of the region, which indicates the angle of the sunlight. For instance, at higher latitudes daytime is longer, on the other hand, sunlight angle is lower which makes solar radiance inefficient during summer.

References

[1]   Raymer, D. P., *Aircraft Design: A ConceptualApproach*, 4th edition, AIAA Education Series, 2006.

[2]   Nicolai L. M., Grant. E. Carichner. *Fundamentals of Aircraft and Airship Design Volume I — Aircraft Design*, AIAA Series, 2010

[3]   Gudmundsson, S., *General Aviation Aircaft Design Applied Methods and Procedures*, BH Series, 2014

[4]   Noth, A., *Design of Solar Powered Airplanes for Continuous Flight*, Ph. D. Dissertation, Autonomous Systems Lab, ETH Zürich, Switzerland, 2008.

[5]   "Solar Impulse." [Online]. Available: http://www.solarimpulse.com, last visited on March 2016.

[6]   "Airfoil profile database." [Online]. Available: http://aerospace.illinois.edu/m-selig/ads.html, last visited on March 2016.

[7]   "Northrop Grumman Corp. Global Hawk." [Online]. Available: http//www.northopgrumman.com/Capabilities/GlobalHawk/pages/default.aspx, last visited on March 2016.

[8]   "Battery University." [Online]. Available: http://batteryuniversity.com/, last visited on March 2016.

[9]   Boucher, R. J., "Sunrise the World's First Solar-Powered Airplane." *Journal of Aircraft* Vol 22, No 10, 1985.

[10]   Romeo, G., Frulla, G., Cestino, E, and Corsino, G., "Design, Aerodynamic, Structural Analysis of Long-Endurance Solar-Powered Stratospheric Platform", *Journal of Aircraft,*pp:1505-1520, 2004.

[11]   Boucher, R. J. , "History of Solar Flight." SAE, and ASME, *20th Joint Propulsion Conference*, Cincinnati, OH, June 11-13, AIAA-1984-1429, 1984.

[12]   "Autonomus Solar Airplane for Mars Exploration", [Online]. Available: http://www.sky-sailor.ethz.ch, last visited on March 2016.

[13]   "Navair Orders 7 Zephyr Ultra-long Endurance UAV's", [Online]. Available: http://www.defenseindustrydaily.com/NAVAIR-Orders-7-Zephyr-Ultra-Long-Endurance-UAVs-05426/, last visited on March 2016.

[14]   Hoerner, S. F., *Fluid Dynamic Drag*, Brick Town, N. J. USA, 1965.

[15]   Altman, A., Ph.D. thesis, A Conceptual Design Methodology for Low Speed High Altitude Long Endurance Unmanned Aerial Vehicles, 2000.

[16]   Duffie, J.A., Beckman, W. A., *Solar energy thermal proceseses*, 4th edition, John Wiley and Sons, Inc, 2013.

[17]   Deperrois, A., XFLR5 Program, [Online]. Available:http://www.xflr5.com/xflr5.htm, 2012, last visited on March 2016.

[18]   Gundlach, J., *Designing Unmanned Aircraft Systems*, AIAA Education Series, 2012.

[19]   Mermer, E., Köker, A., Kurtuluş, D.F., Yılmaz, E., "Design and Performance of Wing Configurations for High Altitude Solar Powered Unmanned Systems,", AIAC- 2013-141 2013.

[20]   Anderson, J. D. Jr., *Aircraft Performance and Design*, McGraw Hill, 1999.

[21]   Office of the Secretary of Defense. "Unmanned Aerial Vehicle Reliability Study." February 2003.

[22]   Keidel, B., "Design of a solar-powered hale aircraft for year-round operation at intermediate latitudes." Proceeding of the RTO symposium on "UV for aerial, ground and naval military ope- rations", Ankara, Turkey, 2000.

[23]   Nickol, Craig, L., *High altitude long endurance uav analysis of alternatives and technology requirements development*. NASA/TP-2007-214861, National Aeronautics and Space Administration, Langley Research Center, Hampton, VA, 2007.

[24]   Montagnier, O., Laurent, B., "Optimization of A Solar-Powered High Altitude Long Endurance UAV." 27th International Congress of Aeronautical Science, Nice France. September 2010.

[25]   Cestino, E. "Design of solar high altitude long endurance aircraft for multi payload & operations." Aerospace science and technology 10.6 (2006): 541-550 2006.

[26]   Roberto, C., Marino, L., "Preliminary Design of a Hybrid Propulsion System For High-Endurance UAV." In: Proceedings of the ASME 2010 International Mechanical Engineering Congress & Exposition IMECE2010, Vancouver, British Columbia, Canada, November 12-18, 2010.

[27]   Roskam, J., *Airplane Design Parts I through VIII*, Darcorporation, 2003

[28]   Gundlach, J., *Designing Unmanned Aircraft Systems: A Comprehensive Approach,* American Institute of Aeronautics & Astronautics Series.2013.

[29]   Harvey, J. R., "Development of a hybrid-electric power-system model for a small surveillance aircraft." 28th International Congress of the Aeronautical Sciences. 2012.

[30]   Flittie, K, Curtin, B., "Pathfinder solar-powered aircraft flight performance", AIAA Atmospheric Flight Mechanics Conference & Exhibit, Boston, 1998.